

The magnetisation of protoplanetary disks

G.T. Birk^{1,2*}, H. Wiechen², A. Kopp³ and H. Lesch^{1,2}

¹ Institut für Astronomie und Astrophysik, Ludwig-Maximilians-Universität München, Germany

² Centre of Interdisciplinary Plasma Science, Garching, Germany

³ Theoretische Physik IV, Ruhr-Universität Bochum, Bochum, Germany

ABSTRACT

The remanent magnetisation of meteorite material in the solar system indicates that magnetic fields of several Gauss are present in the protoplanetary disk. It is shown that such relatively strong magnetic fields can be generated in dusty protoplanetary disks by relative shear motions of the charged dust and the neutral gas components. Self-consistent multi-fluid simulations show that for typical plasma parameters shear flows with collisional momentum transfer between the different components of the dusty plasma result in a very efficient generation of magnetic fields with strengths of about 0.1–1 Gauss on spatial scales of two astronomical units in about one year. Based on the simulations one may predict that future measurements will reveal the strong magnetisation of circumstellar disks around young stellar objects.

Key words: planetary systems: protoplanetary disks – accretion disks – Magnetic fields – circumstellar matter

1 INTRODUCTION

Meteors are commonly considered to be relics of the protoplanetary nebula in our early solar system. Of particular importance in the context of the early evolution of the solar system is the remanent magnetisation of meteorite material that indicates the presence of relatively strong magnetic fields ($B = 1 - 10$ G) in protoplanetary nebula (Levy & Sonett 1978; Sugiura et al. 1979). The formation of meteorite chondrules may also demand for magnetic fields as the relevant energy source (Sonett 1979; Levy & Araki 1989). Thus, one faces the

* E-mail: birk@usm.uni-muenchen.de

question of the origin of such strong magnetic fields in protoplanetary disks. Recent numerical calculations of collapsing magnetised molecular cloud cores have proven that ambipolar diffusion can solve the magnetic flux loss problem of the formation of protostellar objects (Ciolek & Königl 1993; Desch & Mouschovias 2001). The magnetic flux can diffuse to the region around the protostellar object and thus result in a magnetic field of the protoplanetary disk of some 0.1 G (Desch & Mouschovias 2001). The fate of this field after the stellar object has fully evolved and accretion flow in the disk sets in is, however, not clear. In this contribution we consider disk magnetisation in a later stage of the stellar evolution, namely after a stellar object with a dipole magnetic field has formed.

A characteristic feature of partially ionised plasmas is the possibility that magnetic fields can be generated without any seed fields. As shown by (Huba & Fedder 1993) a relative plasma-neutral gas flow with non-vanishing vorticity results inevitably in the generation of magnetic fields. This effect is described by the generalised Ohm's law on the grounds of a multi-fluid description. The magnetisation mechanism works significantly more efficiently in a dusty plasma (Birk et al. 1996; Birk et al. 2001) where the inertia effects and collisional momentum transfer are dominated by the heavy dust grains.

In this contribution we show by means of multi-fluid simulations that relative shear flows lead to a very fast three-dimensional magnetic field self-generation in dusty protoplanetary disks. Magnetic field strengths up to one Gauss are generated on the time scale of 1yr on spatial scales of some astronomical units (AU).

2 SELF-MAGNETISATION OF PROTOPLANETARY ACCRETION DISKS

We consider the following balance equations that govern the low-frequency macroscopic dynamics of a partially ionised dusty plasma (see Birk et al. 1996; Birk et al. 2001)

$$\frac{\partial \rho_d}{\partial t} = -\nabla \cdot (\rho_d \mathbf{v}_d) \quad (1)$$

$$\frac{\partial \rho_i}{\partial t} = -\nabla \cdot (\rho_i \mathbf{v}_i) \quad (2)$$

$$\frac{\partial \rho_n}{\partial t} = -\nabla \cdot (\rho_n \mathbf{v}_n) \quad (3)$$

$$\begin{aligned} \frac{\partial(\rho_d \mathbf{v}_d)}{\partial t} = & -\nabla \cdot (\rho_d \mathbf{v}_d \mathbf{v}_d) - \nabla(p_e + p_i + p_d) + (\rho_i + \rho_d) \mathbf{g} \\ & + (\nabla \times \mathbf{B}) \times \mathbf{B} - \nu_{dn} \rho_d (\mathbf{v}_d - \mathbf{v}_n) \end{aligned}$$

$$- \nu_{in} \rho_i (\mathbf{v}_i - \mathbf{v}_n) - \nu_{en} \rho_e (\mathbf{v}_e - \mathbf{v}_n) \quad (4)$$

$$\begin{aligned} \frac{\partial(\rho_n \mathbf{v}_n)}{\partial t} = & - \nabla \cdot (\rho_n \mathbf{v}_n \mathbf{v}_n) - \nabla p_n + \rho_n \mathbf{g} \\ & + \nu_{dn} \rho_d (\mathbf{v}_d - \mathbf{v}_n) + \nu_{in} \rho_i (\mathbf{v}_i - \mathbf{v}_n) \\ & + \nu_{en} \rho_e (\mathbf{v}_e - \mathbf{v}_n) \end{aligned} \quad (5)$$

$$\begin{aligned} \frac{1}{\gamma_e - 1} \frac{\partial p_e}{\partial t} = & - \frac{1}{\gamma_e - 1} \nabla \cdot (p_e \mathbf{v}_e) - p_e \nabla \cdot \mathbf{v}_e + \rho_n \nu_{ne} (\mathbf{v}_e - \mathbf{v}_n)^2 \\ & - 2 \frac{\rho_d \nu_{de}}{m_d} \left(\frac{k_B T_e}{\gamma_e - 1} - \frac{k_B T_d}{\gamma_d - 1} \right) - 2 \frac{\rho_i \nu_{ie}}{m_i} \left(\frac{k_B T_e}{\gamma_e - 1} - \frac{k_B T_i}{\gamma_i - 1} \right) \\ & - 2 \frac{\rho_n \nu_{ne}}{m_n} \left(\frac{k_B T_e}{\gamma_e - 1} - \frac{k_B T_n}{\gamma_n - 1} \right) + \rho_d \nu_{de} (\mathbf{v}_e - \mathbf{v}_d)^2 \\ & + \rho_i \nu_{ie} (\mathbf{v}_e - \mathbf{v}_i)^2 \end{aligned} \quad (6)$$

$$\begin{aligned} \frac{1}{\gamma_i - 1} \frac{\partial p_i}{\partial t} = & - \frac{1}{\gamma_i - 1} \nabla \cdot (p_i \mathbf{v}_i) - p_i \nabla \cdot \mathbf{v}_i + \frac{m_n}{m_i + m_n} \rho_i \nu_{in} (\mathbf{v}_i - \mathbf{v}_n)^2 \\ & + \frac{m_d}{m_d + m_i} \rho_i \nu_{id} (\mathbf{v}_i - \mathbf{v}_d)^2 - 2 \frac{\rho_i \nu_{in}}{m_i + m_n} \left(\frac{k_B T_i}{\gamma_i - 1} - \frac{k_B T_n}{\gamma_n - 1} \right) \\ & - 2 \frac{\rho_i \nu_{id}}{m_i + m_d} \left(\frac{k_B T_i}{\gamma_i - 1} - \frac{k_B T_d}{\gamma_d - 1} \right) - 2 \frac{\rho_i \nu_{ie}}{m_i} \left(\frac{k_B T_i}{\gamma_i - 1} - \frac{k_B T_e}{\gamma_e - 1} \right) \\ & + \frac{m_e}{m_i} \rho_i \nu_{ie} (\mathbf{v}_i - \mathbf{v}_e)^2 \end{aligned} \quad (7)$$

$$\begin{aligned} \frac{1}{\gamma_d - 1} \frac{\partial p_d}{\partial t} = & - \frac{1}{\gamma_d - 1} \nabla \cdot (p_d \mathbf{v}_d) - p_d \nabla \cdot \mathbf{v}_d + \frac{m_e}{m_d} \rho_d \nu_{de} (\mathbf{v}_d - \mathbf{v}_e)^2 \\ & + \frac{m_i}{m_i + m_d} \rho_d \nu_{di} (\mathbf{v}_d - \mathbf{v}_i)^2 + \frac{m_n}{m_n + m_d} \rho_d \nu_{dn} (\mathbf{v}_d - \mathbf{v}_n)^2 \\ & - 2 \frac{\rho_d \nu_{di}}{m_i + m_d} \left(\frac{k_B T_d}{\gamma_d - 1} - \frac{k_B T_i}{\gamma_i - 1} \right) - 2 \frac{\rho_d \nu_{dn}}{m_n + m_d} \left(\frac{k_B T_d}{\gamma_d - 1} - \frac{k_B T_n}{\gamma_n - 1} \right) \\ & - 2 \frac{\rho_d \nu_{de}}{m_d} \left(\frac{k_B T_d}{\gamma_d - 1} - \frac{k_B T_e}{\gamma_e - 1} \right) \end{aligned} \quad (8)$$

$$\begin{aligned} \frac{1}{\gamma_n - 1} \frac{\partial p_n}{\partial t} = & - \frac{1}{\gamma_n - 1} \nabla \cdot (p_n \mathbf{v}_n) - p_n \nabla \cdot \mathbf{v}_n \\ & + \frac{m_i}{m_i + m_n} \rho_n \nu_{ni} (\mathbf{v}_i - \mathbf{v}_n)^2 + \frac{m_e}{m_n} \rho_n \nu_{ne} (\mathbf{v}_e - \mathbf{v}_n)^2 \\ & + \frac{m_d}{m_n + m_d} \rho_n \nu_{nd} (\mathbf{v}_n - \mathbf{v}_d)^2 - 2 \frac{\rho_n \nu_{ni}}{m_i + m_n} \left(\frac{k_B T_n}{\gamma_n - 1} - \frac{k_B T_i}{\gamma_i - 1} \right) \\ & - 2 \frac{\rho_n \nu_{nd}}{m_n + m_d} \left(\frac{k_B T_n}{\gamma_n - 1} - \frac{k_B T_d}{\gamma_d - 1} \right) \\ & - 2 \frac{\rho_n \nu_{ne}}{m_n} \left(\frac{k_B T_n}{\gamma_n - 1} - \frac{k_B T_e}{\gamma_e - 1} \right) \end{aligned} \quad (9)$$

$$\begin{aligned} \frac{\partial \mathbf{B}}{\partial t} = & - \frac{m_i c}{e} \nabla \times \left(\frac{\nabla p_i}{\rho_i} \right) + \frac{m_i}{m_d} z_d \nabla \times \left(\frac{\rho_d}{\rho_i} \mathbf{v}_d \times \mathbf{B} \right) \\ & + \frac{m_i c}{4\pi e} \nabla \times \left(\left(\frac{\nabla \times \mathbf{B}}{\rho_i} \right) \times \mathbf{B} \right) - \eta \Delta \mathbf{B} \end{aligned}$$

$$- \frac{m_i c}{e} \nabla \times \left[\frac{n_d}{n_i} \left(\left(z_d - \frac{n_i}{n_d} \right) \nu_{id} + z_d \nu_{in} \right) \mathbf{v}_d - \nu_{in} \mathbf{v}_n \right] \quad (10)$$

where ρ_α , \mathbf{v}_α , m_α , p_α and \mathbf{B} are the respective ($\alpha = d, i, e, n$) mass density, bulk velocity, particle mass (the ions are assumed to be protons), thermal pressure ($p_\alpha = \rho_\alpha k_B T_\alpha / m_\alpha$, where k_B is the Boltzmann constant and T_α is the temperature) and magnetic field strength. The adiabatic ratios of specific heats are chosen as $\gamma_\alpha = 5/3$. The collision frequencies for collisions (elastic collisions as well as charge exchange) between species α and β are denoted by $\nu_{\alpha\beta}$ and satisfy $\rho_\alpha \nu_{\alpha\beta} = \rho_\beta \nu_{\beta\alpha}$. By η the collisional diffusivity ($\eta = m_i c^2 (\nu_{id} + \nu_{in}) / 4\pi n_i e^2$) is denoted. Ionisation and recombination are neglected in the present context. The electron density is calculated from the quasi-neutrality condition ($\rho_i / m_i - \rho_e / m_e - z_d \rho_d / m_d = 0$) where z_d is the negative dust charge number. The momentum transfer equations that include external gravitational forces with the acceleration \mathbf{g} are formulated as the sum of the balance equations of all charged components under the assumption of inertialess ions and electrons (as compared to the massive dust grains). Most important for the self-generation of magnetic fields is the induction equation (see also Ciolek & Mouschovias, 1993) which may be derived from the inertialess ion momentum equation. The final term in Eq. (10) is the relevant magnetic field self-generation term. The mass, momentum and pressure balance equations as well as the induction equation are integrated numerically by the DENISIS code (Schröer et al. 1998) under the assumption of ionisation equilibrium. This explicit finite differences code is based on a modified Leapfrog algorithm. Extensive tests and applications of the code can be found in the papers by Schröer et al. (1998), Birk et al. (2001) and Birk and Wiechen (2002).

Although the present study is motivated by the local information of the magnetised meteorite material in the solar system we assume that our solar system is a standard case for normal stellar systems. Thus, in the following we consider a simple protoplanetary accretion disk model consisting of electrons, protons, neutrals and charged dust grains using typical dynamical parameters for circumstellar disks around T Tauri stars (Montmerle 1991; Königl 1994). In particular, we choose the following parameters: $n_i = 1.01 n_d = 0.1 n_n = 10^{12} \text{ cm}^{-3}$, $z_d = 1$, $m_d = 100 m_i$, and for the temperatures $T_n = T_i = T_d = 500 \text{ K}$. The ion- neutral collision frequencies can be estimated as (e.g. Krall & Trivelpiece 1986) $\nu_{in} \approx \sigma(T_i) n_n \sqrt{k T_i / m_i}$ where k is the Boltzmann constant and σ denotes the cross section. The latter depends on the ion temperature in a way that results in a collision frequency that is independent on the ion temperature (for more details on the collision theory see, e.g., Mitchner & Kruger 1973).

We use $\sigma = 5 \cdot 10^{-15} \text{ cm}^2$ as constant approximation of sufficient accuracy in our context. The ion-dust collision frequency is $\nu_{id} \approx 4\sqrt{2\pi}n_dz_d^2e^4\ln(\lambda_D/a)/3m_i^{1/2}(kT_i)^{3/2}$ (Benkadda et al. 1996) where $\lambda_D = \sqrt{kT_d/4\pi n_dz_d^2e^2}$ denotes the dust Debye screening length. For the dust grain size we choose $a = 10^{-6} \text{ cm}$. The actual choice of the grain size has no significant influence on the induction equation, since a only enters in the logarithm of the formula for the ion-dust frequency and does not play an important role for the magnetic field generation due to the strong electron depletion ($z_d - n_i/n_d \approx 0$ in Eq. 10). On the other hand, the momentum transfer between the dust and the neutral fluid components depends on the grain radius. However, the continuous acceleration (accretion flow) guarantees a finite relative dust-neutral shear flow. Without this energy source larger dust grains would result in faster saturation and weaker generated magnetic fields.

Within a region of 10 AU we consider an initially homogenous protoplanetary disk in which the dust grains as well as the ions are chosen to be in corotation within a region of about 1 AU (Fig. 1, upper plot). The corotation of the charged dust grains is caused by a stellar dipole field. The neutrals do not couple directly to the magnetic field but via momentum transfer with the charged particles. Outside this corotation radius the dust is in Keplerian motion (Li 1996). The neutral gas is assumed to be in Keplerian motion with the exception of a very inner region of 0.2 AU where the neutral gas is assumed to be in corotation to avoid singularities (Fig. 1, lower plot). The typical velocities near the transition regions between corotation and Keplerian motion are about $1 \cdot 10^6 \text{ cm s}^{-1}$ for the dust and $1.5 \cdot 10^7 \text{ cm s}^{-1}$ for the neutral gas, respectively.

The orders of magnitude of these velocities are in a rough agreement with a central mass object of about 2 solar masses, so that we include an external gravitational force corresponding to such a central mass. The initial configuration is characterised by the immediate onset of idealised accretion flow rather than to be in a stationary state. The gravitational field is the ultimate energy source for the generation of the magnetic field.

The simulation box is given by $x \in [-25, 25]$, $y \in [-25, 25]$ and $z \in [0, 10]$ in units of 0.2 AU. The equidistant grid is resolved by $77 \times 77 \times 31$ grid points. The boundary conditions are symmetric at all boundaries, i.e. the values of the scalar quantities and vector components at the numerical boundaries correspond to the values at the respective last inner grid points.

As the upper plot of Fig. 2 indicates, a swirl-like dust flow in the central disk in the x - y -plane has built up after 0.7 yr. The curl of the relative dust-neutral gas flow (Fig. 2,

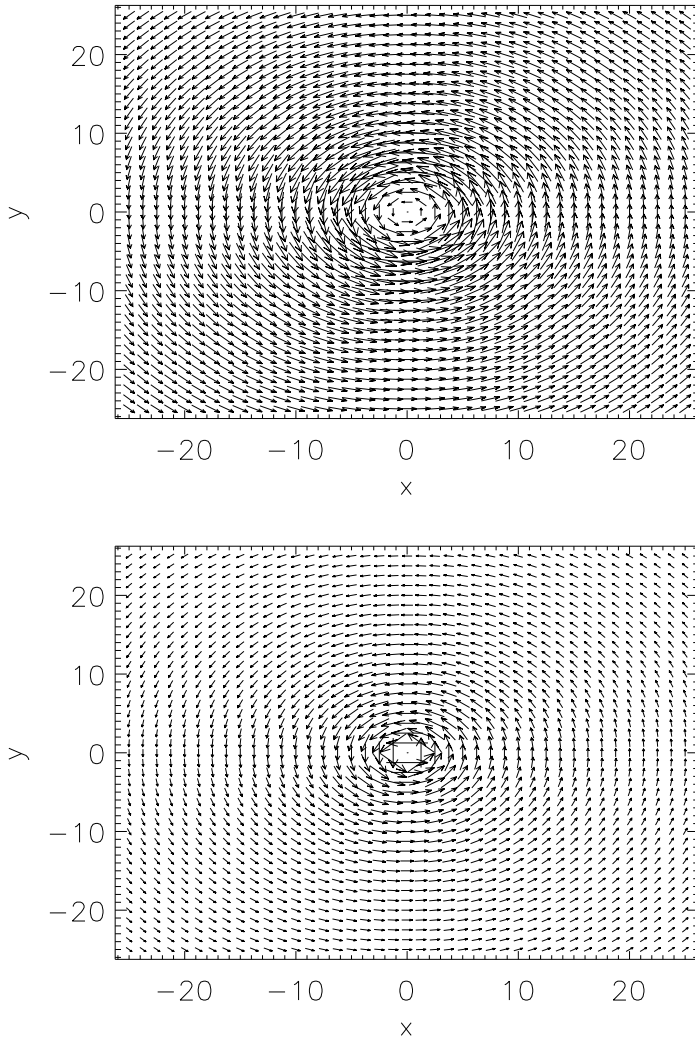


Figure 1. The initial dust (upper plot) and neutral gas (lower plot) velocity patterns. The velocity field is initially invariant in the z -direction, i.e. perpendicular to the disk. The spatial scales are given in units of 0.2 AU.

lower plot) is sustained by the gravitational pull and results in an ongoing magnetisation of the disk.

The magnetic field after $t = 0.7$ yr and $t = 1.4$ yr is shown in Figs. 3 and 4, respectively. The strengths of the different field components are roughly comparable. After $t = 0.7$ yr, the amplitude of $B_z = 0.8$ G is 5 times the amplitudes of B_x and B_y and after $t = 1.4$ yr, the factor is about 2 ($B_z = 1.2$ G). The field generation is caused not only by the poloidal flows that develop from the initial configuration but also by vertical relative shear flows arising in the dusty accretion disk.

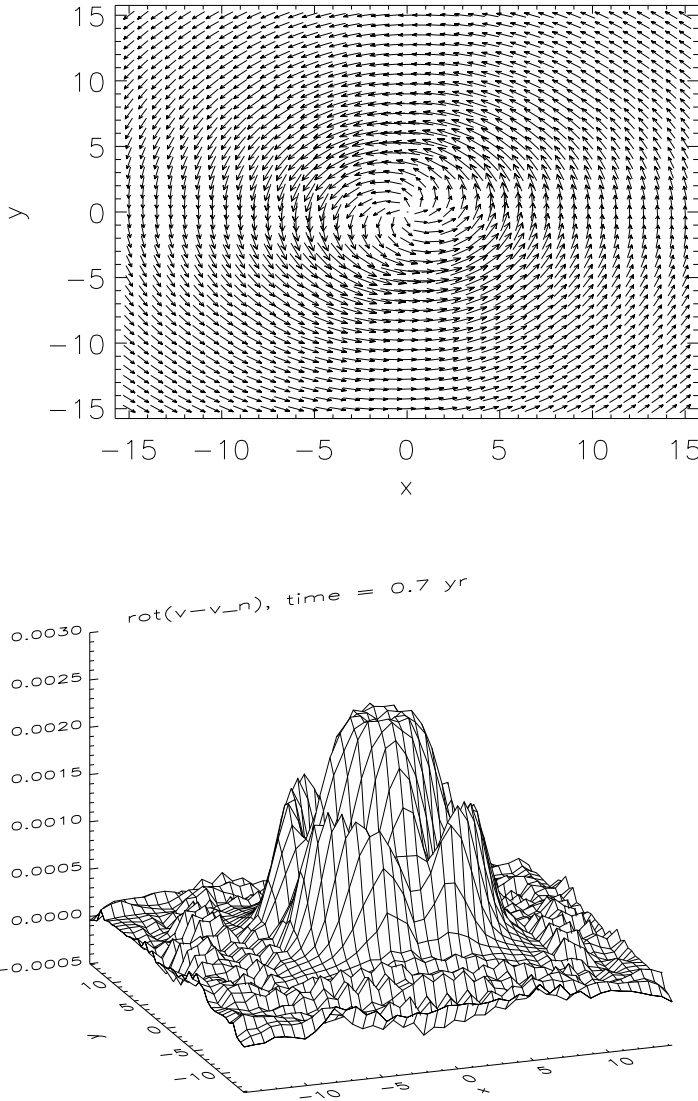


Figure 2. The poloidal dust velocity patterns at the middle of the disk (as far as the vertical extension goes) and the z -component of the curl of the relative dust-neutral gas flows after $t = 0.7$ yr. The amplitude is measured in units of the initial amplitude of v_{dx} .

The magnetic energy density $W_B = B^2/8\pi$ at different heights of the disk are shown in Fig. 5. Obviously, the inner part of the disk is completely magnetised in all three dimensions.

Since the ultimate source of the self-magnetisation is the stellar gravitation the process lasts as long as the accretion flow in the circumstellar disk is present. The numerical simulation, however, fails when the central density gradient becomes too steep (after about 200 dynamical times). This is a consequence of our simulation approach that does not properly deal with the accretion of matter (loss of plasma to the stellar object) and the formation of

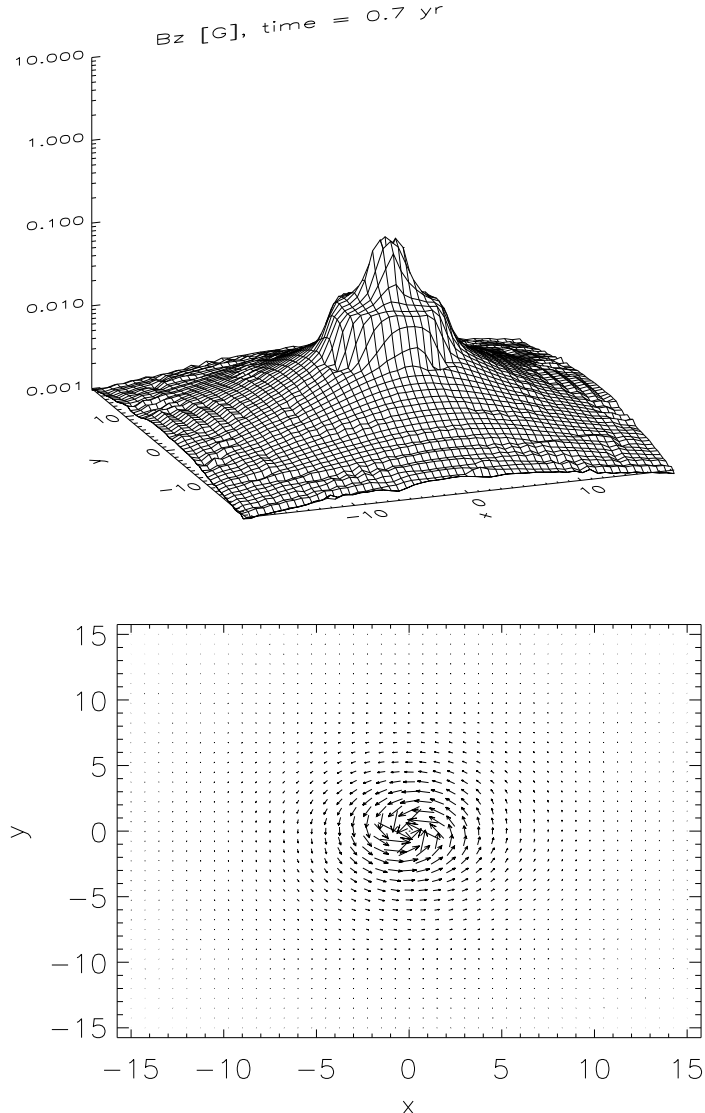


Figure 3. The magnetic field after $t = 0.7\text{yr}$. The upper plot shows the z -component of the magnetic field and the lower one the poloidal magnetic field at $z = 5$.

bipolar jets. A global multi-fluid model including all relevant physics is clearly beyond the scope of the present state of the art.

3 DISCUSSION

We studied the magnetisation of protoplanetary disks that consist of dusty plasmas. Different from previous studies on the magnetisation of the environment of collapsing molecular cloud cores (Ciolek & Königl 1993; Desch & Mouschovias 2001) we dwell on the magnetic field generation in fully developed accretion disks. The process is driven by accretion, i.e. the ultimate source of energy for the magnetic field is the stellar gravitational field, it results in

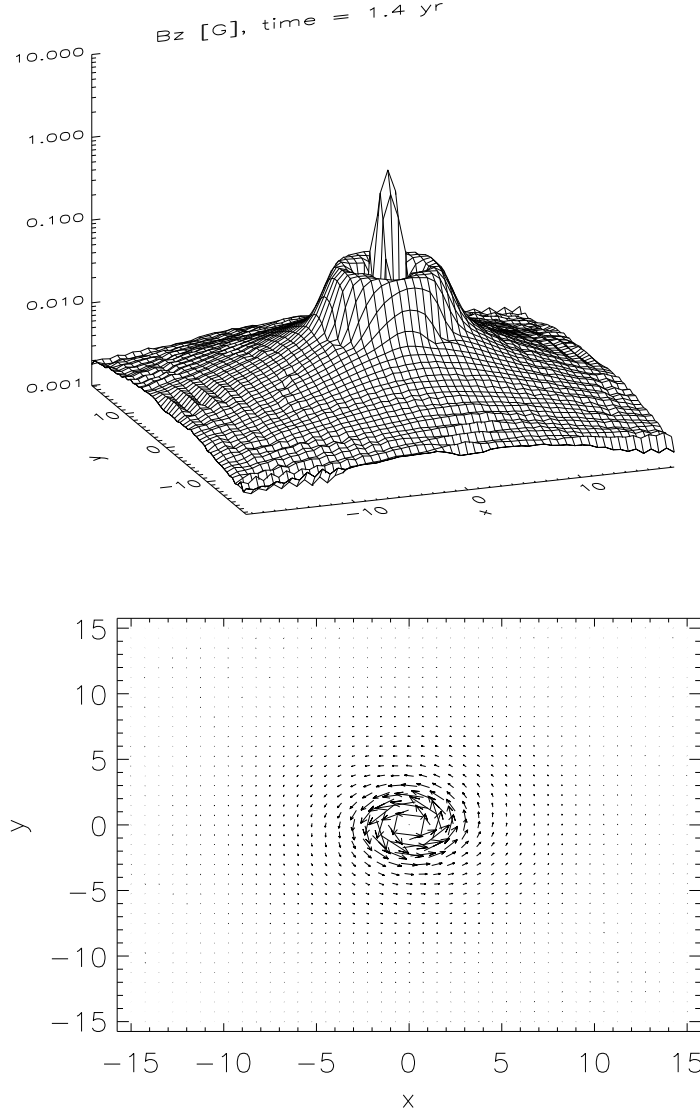


Figure 4. The magnetic field after $t = 1.4\text{yr}$. The upper plot shows the z -component of the magnetic field and the lower one the poloidal magnetic field at $z = 5$.

an ordered poloidal magnetic field of some Gauss. It is a very fast and efficient mechanism of field generation. Also it is a process of permanent magnetisation as long as some accretion flow is present.

The numerical simulations show that magnetic fields are generated in circumstellar dusty disks by macroscopic relative shear motions between the different species. This self-magnetisation mechanism that works in addition to the formation of turbulent magnetic fields due to the interaction of the stellar field with a turbulent accretion disk (Bardou & Heyvaerts 1996).

We note that in our studies we did not include a stellar magnetic field explicitly. Such a field should give rise to a (sheared) wind component close to the star and thus, possibly to

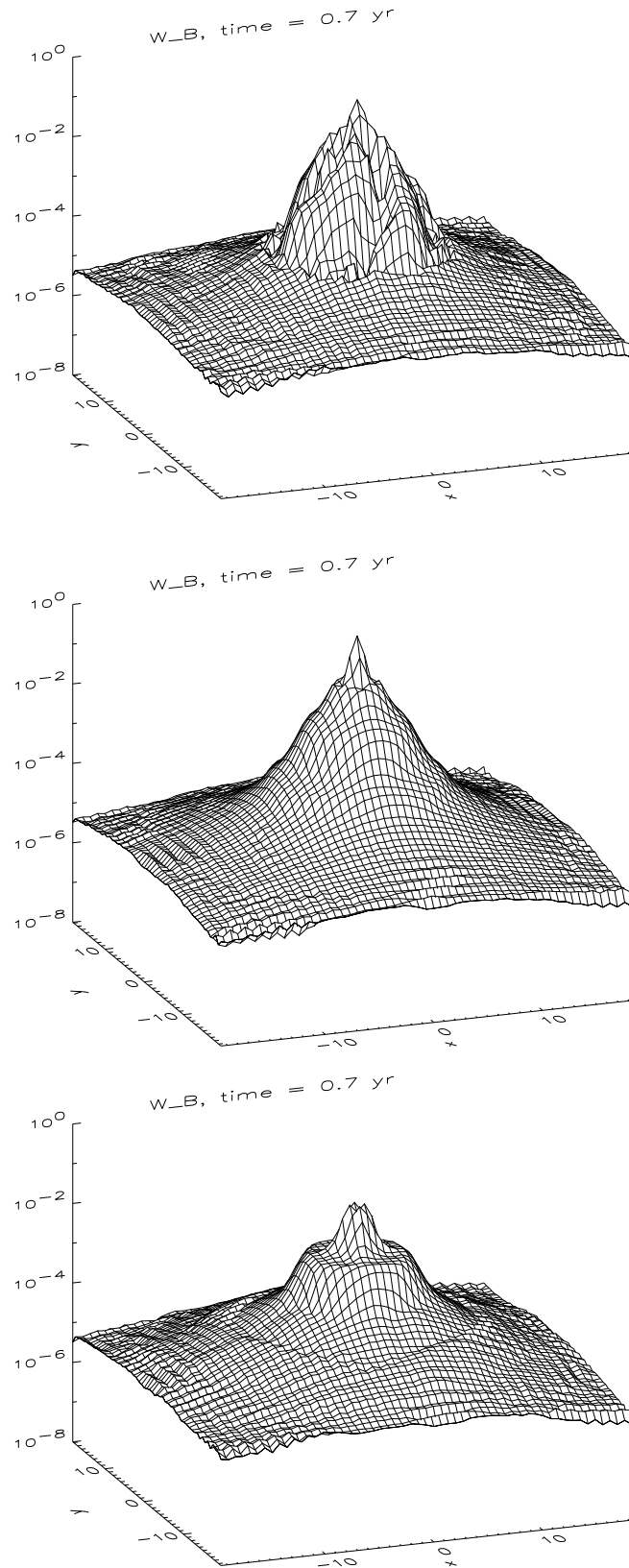


Figure 5. The magnetic field energy density (W_B) at different heights ($z = 1.4$, upper plot; $z = 5$, middle plot; $z = 8.6$ lower plot) of the protoplanetary disk.

the further magnetisation of a significant fraction of the magnetosphere. In this contribution we concentrated on the generation of magnetic fields in the accretion disks. Further studies that include stellar fields are a promising task for the future.

In our simulations we did not include a gap between the central stellar object and the disk for technical reasons. However, since we were interested in the *in situ* magnetisation of the disk material this idealisation does not influence our findings.

A further idealisation of our study is the initial density homogeneity of the disk. However, in the course of the dynamical evolution radial profiles form in all fluid components due to the external gravitation. More realistic density profiles perpendicular to the disk would demand for the inclusion of self-gravitation. The inclusion of this further energy source that also may contribute to the self-magnetisation of the disk is beyond the scope of the present investigations but could be of interest for future numerical modelling. Parameter studies, however, have shown that the efficiency of the process of magnetisation is not significantly influenced by the variation of the initial number densities over a wide parameter range.

Given the uncertainties of the actual plasma parameters the high efficiency of the discussed magnetisation guarantees that protoplanetary disks are expected to generate their own magnetic fields of the order of 0.1 – 1 Gauss. In the presence of a small radial magnetic field component the Balbus-Hawley shear instability (Balbus & Hawley 1991) can, in principle, result in a faster than linear growth of the poloidal magnetic field component provided the appropriate onset criterion is fulfilled. This criterion, however, is not known for multifluid systems. On the other hand, localized reconnection may result in a redistribution of magnetic flux. Investigations on this process are beyond the scope of the present contribution and will be considered in further more detailed work.

If circumstellar disks carry their own significant magnetic fields, dynamic phenomena in the coupled star-disk system are rather complex. The disk field should influence characteristic phenomena as, e.g., accretion, winds and jets and magnetic activity, significantly.

REFERENCES

- Balbus, S.A., Hawley, J.F., 1991, *ApJ*, 376, 214
- Bardou, A., Heyvaerts, J., 1996, *A& A*, 307, 1009
- Benkadda, S., Gabbai, P., Tsytovich, V.N., Verga, A., 1996, *Phys. Rev. E*, 53, 2717
- Birk, G.T., Kopp, A., Shukla, P.K., 1996, *Phys. Plasmas*, 3, 3564

Birk, G.T., Kopp, A., Lesch, H., 2001, *J. Plasma Phys.*, 66, 213

Birk, G.T., Wiechen, H., 2002, *Phys. Plasmas*, 9, 964

Ciolek, G.E., Mouschovias, T.C., 1993, *ApJ*, 418, 774

Ciolek, G.E., KÖnigl, A., 1998, *ApJ*, 504, 257

Desch, S.J., Mouschovias, T.Ch., 2001, *ApJ*, 550, 314

Huba, J.D., Fedder, J., 1993, *Phys. Fluids B*, 5, 3779

Königl, A., 1994, in *Theory of Accretion Disks*, edited by W.J. Duschl et al. (Kluwer, Dordrecht, 1994), p. 53

Kopp, A., Schröer, A., Birk, G.T., Shukla, P.K., 1998, *Phys. Plasmas*, 4, 4414

Krall, N.A., Trivelpiece, A.W., 1986, *Principles of Plasma Physics*, San Francisco Press, p.321

Levy, E.H., Sonett, C.P., 1978, Meteorite Magnetism and Early Solar System Magnetic Fields, in *Protostars & Planets*, edited by T. Gehrels (Arizona Press, Tucson, 1978), p. 516.

Levy, E.H., Araki, S., 1989, *Icarus* 81, 74

Li, J., 1996, *ApJ*, 456, 696

Mitchner, M., Kruger, C.H., 1973, *Partially Ionized Gases*, Wiley, New York, ch.5

Montmerle, T., 1991, in *The Physics of Star Formation* edited by C.J. Lada & N.D. Kylatis (Kluwer, Dordrecht, 1991), p. 675

Schröer, A., Birk, G.T., Kopp, A., 1998, *Comp. Phys. Comm.*, 112, 7

Sonett, C.P., 1979, *Geophys. Res. Lett.*, 8, 677

Sugiura, N., Lanoix, M., Strangeway, D.W., 1979, *Phys. Earth Planet. Inter.*, 20, 342

This paper has been typeset from a *TeX/ L^AT_EX* file prepared by the author.